



OPEN

Transcription activator-like effector
nuclease-mediated transduction of
exogenous gene into *IL2RG* locusSUBJECT AREAS:
TARGETED GENE REPAIR
GENETIC VECTORSYohei Matsubara^{1,2*}, Tomoki Chiba^{1*}, Kenichi Kashimada², Tomohiro Morio², Shuji Takada³,
Shuki Mizutani² & Hiroshi Asahara^{1,3,4,5}Received
6 January 2014Accepted
2 May 2014Published
23 May 2014

¹Department of Systems BioMedicine, Tokyo Medical and Dental University Graduate School of Medical and Dental Sciences, Tokyo 113-8510, Japan, ²Department of Pediatrics and Developmental Biology, Tokyo Medical and Dental University Graduate School of Medical and Dental Sciences, Tokyo 113-8510, Japan, ³Department of Systems BioMedicine, National Research Institute for Child Health and Development, Tokyo 157-8535, Japan, ⁴CREST, Japan Science and Technology Agency (JST), Saitama 332-0012, Japan, ⁵Department of Molecular and Experimental Medicine, The Scripps research Institute, La Jolla, CA 92037, USA.

Correspondence and
requests for materials
should be addressed to
H.A. (asahara.syst@
tmd.ac.jp)

* These authors
contributed equally to
this work.

X-linked severe combined immunodeficiency (SCID-X1) caused by mutations in interleukin 2 receptor gamma (*IL2RG*) gene threatens the survival of affected boys during the first year of life unless hematopoietic stem cell transplantation is provided. Although viral vector-mediated gene therapy has been successfully performed in patients with no HLA-matched donors, leukemia caused by vector-mediated insertional mutagenesis has been reported in some individuals. Transcription activator-like effector nuclease (TALEN) is an artificial sequence-specific endonuclease that is expected to revolutionize the precise correction of disease-causing mutations and eliminate the risk of insertional mutagenesis. Here, we report TALEN-mediated genome editing of the *IL2RG* locus. We transfected TALENs along with a targeting vector into Jurkat cells, and we confirmed the precise introduction of the exogenous gene into the *IL2RG* locus. In addition, we found that the length of homology arm in the targeting vector influenced the efficiency of TALEN-mediated homologous recombination.

X-linked severe combined immunodeficiency (SCID-X1) is the most common form of combined immunodeficiency; it is caused by mutations in the X chromosome-linked interleukin 2 receptor gamma gene (*IL2RG*)¹. *IL2RG*, also known as CD132, is a common cytokine receptor subunit for IL-2, IL-4, IL-7, IL-9, IL-15, and IL-21. Lack of *IL2RG* function results in loss of multiple cytokine activities, leading to absence of T and natural killer (NK) lymphocytes and nonfunctional B lymphocytes. Most SCID-X1 patients die during infancy unless reconstitution of the immune system is achieved through hematopoietic stem cell (HSC) transplantation or gene therapy².

Bone marrow transplantation (BMT) is a curative treatment for SCID-X1. In spite of improvements in transplantation protocols and the introduction of other sources of stem cells such as umbilical cord blood, BMT is associated with serious risks as a result of chemotherapy conditioning regimens, graft-versus-host disease (GVHD), and related infections. Furthermore, only a small percentage of SCID-X1 patients receive BMT owing to a shortage of human leukocyte antigen (HLA)-matched donors.

Gene therapy using viral vectors to transduce therapeutic *IL2RG* into autologous CD34⁺ bone marrow cells has been successful for immune reconstitution for some individuals, resulting in long-term correction of the SCID-X1 phenotype^{3–5}. However, some patients developed T-cell acute lymphoblastic leukemia within 2.5–5 years after gene therapy, one of whom died^{6–9}. Patients' blast cells showed retrovirus vector integration in close proximity to the proto-oncogenes *LMO2*, *CCND2*, and *BMI1*, thus leading to aberrant transcription and expression of these genes^{10–12}. Therefore, gene targeting is needed to eliminate the risks posed by random integration of viral vectors.

Gene targeting based on homologous recombination has been widely used in genetic research; however, its efficiency remains very low. Similarly, therapeutic genes do not undergo homologous recombination at the mutated locus¹³. Homologous recombination is primarily involved in the repair chromosomal double-strand breaks (DSBs), a process known as homology directed repair (HDR)¹⁴. In the absence of homologous donor DNAs, DSBs are repaired by non-homologous end-joining (NHEJ), which frequently results in small insertions and/or deletions (indels). Induction of artificial DSB would significantly improve the efficiency of homologous recombination.

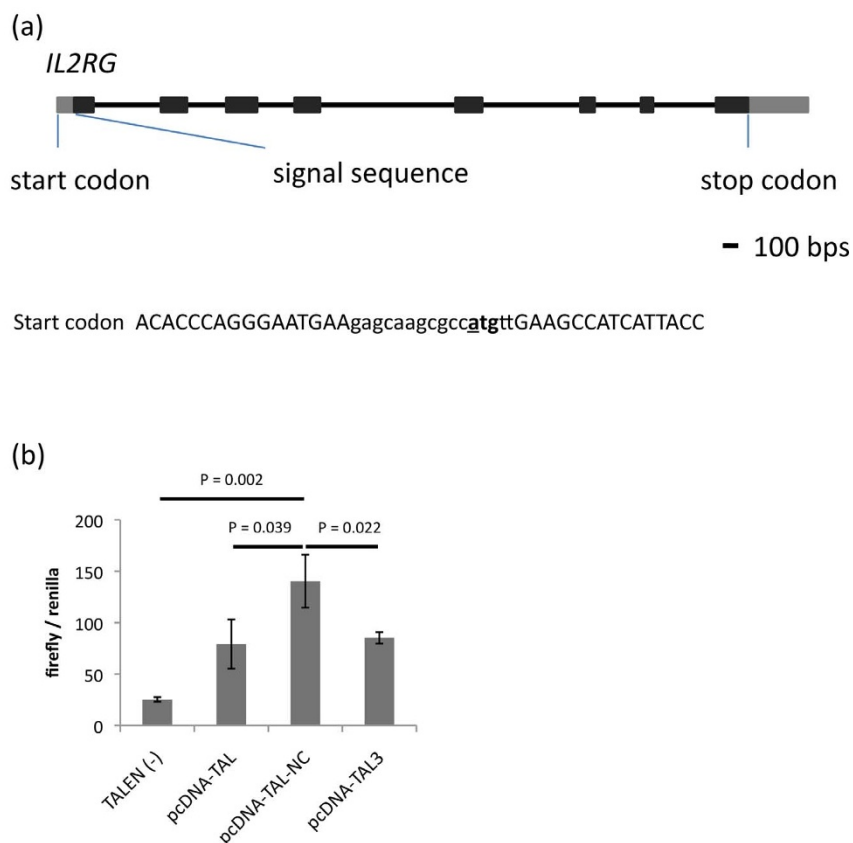


Figure 1 | TALEN design for inducing DSBs in the endogenous *IL2RG* gene in Jurkat cells. (a) Schematic of the TALEN target site at the *IL2RG* start codon in Jurkat cells. *IL2RG* contains eight exons. The binding sites for the TALEN pair used in this study are shown in capital letters, the spacer sequence is indicated in small letters, the start codon (ATG) is in bold, and the TALEN target designed by ZiFit in the spacer sequence is underlined. (b) Functional evaluation of engineered TALENs using the SSA assay. HEK293T cells were transfected with the SSA reporter vector, pRL-TK reference vector, and TALEN expression vectors. After 48 h, a luciferase assay was performed. Data are shown as mean \pm SD (n = 3).

Recently, genome editing technologies such as zinc-finger nuclease (ZFN) and transcription activator-like effector nuclease (TALEN) have enabled the introduction of site-specific DSBs into DNA. ZFNs consist of a DNA-binding domain and a *FokI* endonuclease domain. Each DNA-binding domain recognizes 3–4 DNA bp (nucleotide triplets). Pairs of ZFNs are required to induce DSB in a target locus because the *FokI* cleavage domain is only enzymatically active as a dimer¹⁵. ZFN-induced DSBs were initially shown to enhance gene targeting frequencies in *Drosophila*¹⁶. This was soon followed by endogenous gene correction of *IL2RG* by ZFN in SCID-X1 cells¹⁷. However, ZFN have not become widely used, as some nucleotide triplets lack specific DNA recognition domains, and engineering of ZFN is time consuming, laborious, and intricate¹⁸.

TALEN technologies have also been developed to generate site-specific DSBs¹⁹. TALEN is a sequence-specific endonuclease that consists of a transcription activator-like effector (TALE) and a *FokI* endonuclease. TALE is a DNA-binding protein that has a highly conserved central region with tandem repeat units of 34 amino acids. The base preference for each repeat unit is determined by two amino acid residues called the repeat-variable di-residue (RVD), which recognizes one specific nucleotide in the target DNA. Arrays of DNA-binding repeat units can be customized for targeting specific DNA sequences. As with ZFNs, dimerization of two TALENs on targeted specific sequences in a genome results in *FokI*-dependent introduction of DSBs, stimulating HDR and NHEJ repair mechanisms^{20–22}. In contrast to ZFNs, the design and construction of TALENs is rapid, affordable, and efficient.

Gene therapy without the risk of vector-related insertional mutagenic events is desired for patients who lack HLA-matched donors.

Genome editing is an ideal technique to correct mutations in disease-causing genes. Here, we report TALEN-mediated genome editing and introduction of a reporter gene into the *IL2RG* locus in Jurkat cells.

Results

TALEN design for inducing DSBs at the endogenous human *IL2RG* gene. To induce mutations in *IL2RG*, we targeted the translational start codon of *IL2RG* (Figure 1a). Nucleotide sequences targeted by TALENs were designed using the ZiFit program, and DNA recognition modules were assembled with the Golden Gate method^{23,24}. Assembled modules were cloned into three different expression vectors (pcDNA-TAL, pcDNA-TAL-NC, and pcDNA-TAL3), which differed on the basis of the N- and C-terminal backbone regions of the TALE protein. We examined the nuclease activity of TALENs with different backbones by using the SSA assay²⁴. All three TALENs showed increased luciferase activity induced by DSB-directed nucleotide repair (Figure 1b). Among these, TALENs with the TAL-NC backbone showed highest activity compared to those with TAL and TAL3 backbones. This result suggested that N- and/or C-terminal domains of TALEN are crucial for activity and that the TAL-NC backbone, which is the shortest one tested, was suitable to induce mutation. Therefore, we used the TALEN with the TAL-NC backbone targeting the *IL2RG* start codon for our experiments.

Targeted genomic insertion-deletion at the *IL2RG* locus in Jurkat cells. To examine whether DSB and subsequent NHEJ-directed mutations could be induced in the genome, Jurkat cells, which are



established as a cell line derived from a 14-year-old boy with acute lymphoblastic leukemia and have only a single copy of X chromosome-linked *IL2RG*²⁵, were transfected with plasmids expressing TALENs by electroporation. Five days after electroporation, genomic DNA was extracted for the T7 endonuclease assay. As shown in Figure 2a, cleaved DNAs appeared in Jurkat cells transfected with TAL-NC TALENs, but not in cells transfected with TAL3 TALENs. This finding indicated that TALENs with the TAL-NC backbone were able to induce mutations around the translational initiation site of the *IL2RG* locus. Next, we examined mutations in individual clones that had been isolated by limiting dilution. Sequencing analysis of cloned Jurkat cells revealed that nucleotide deletions were present near the translational initiation site of the *IL2RG* locus and that individual clones had different mutations (Figure 2b). Mutation ratios ranged from 4.8% to 13.3% (Table 1). Furthermore, flow cytometric analysis demonstrated that *IL2RG* protein expression on the cell surface was absent in clones del-2, del-3, and del-4, all of which had deletions in the region containing the translational start codon (Figure 2c). Although clone del-1 contained a deletion of 2-nucleotides, the translational initiation codon remained intact, resulting in similar expression of *IL2RG* compared to wild-type cells. To evaluate the response to IL-2 in the mutated Jurkat cells, we stimulated the cells with PMA and ionomycin in the presence of exogenous IL-2 and analyzed the expression of *BCL2*, which is known to be a downstream target of IL-2 signaling²⁶. The expression of *BCL2* increased by more than two fold after stimulation in wild-type Jurkat cells (Figure 2d). On the other hand, *BCL2* expression did not increase in the mutated cells (Figure 2d). No significant difference in endogenous *IL2* expression of each clone was observed after stimulation (data not shown). In summary, we successfully induced mutation in the *IL2RG* locus by TALEN-mediated genome editing and showed that the mutated cells lost *IL2RG* protein expression and response to IL-2.

Targeted knock-in at the *IL2RG* locus. Because TALENs targeting the start codon were shown to induce DSBs in the *IL2RG* locus, we attempted to induce the HDR. Long and short homology arms were cloned into the targeting vector, which harbored the gene for the Venus fluorescent protein (a brighter variant of the yellow fluorescent protein)²⁷, and a loxP-flanked Neomycin resistance cassette. The 5' end of the DT-A negative selectable marker was also inserted downstream of exon 6 (Figure 3a and Figure S1). Thus, it was expected that fluorescence from Venus expression, driven by the *IL2RG* promoter, would be detectable by TALEN-mediated DSB and subsequent HDR. TALENs and linearized targeting vector were co-transfected into Jurkat cells by electroporation. Transfected cells were selected in G418-containing medium, and single-cell cloning was performed by limiting dilution. Flow cytometric analysis of individual clones revealed that the majority of Jurkat cells co-transfected with TALENs and targeting vector expressed Venus (clones KI 1–4), while only one clone (KI 5) showed high levels of Venus (Venus^{hi}). Southern blot analysis clearly indicated that the gene encoding for Venus was knocked-in at the *IL2RG* locus (Figure 3c). However, clone KI 5 (Venus^{hi}) showed a band corresponding to wild-type cells, as well as additional bands. These data suggested that targeting vectors were randomly integrated into the genome and that Venus expression in the Venus^{hi} clone was driven by adjacent transcriptional activity. We then tested whether the targeting vector with shorter homology arms could also induce HDR. We constructed two novel targeting vectors (pVenus-M and pVenus-S) with shorter homology arms. pVenus-M has a 3000 bp 5' homology arm and a 2000 bp 3' homology arm, while pVenus-S has homology arms of 1000 bp each. Jurkat cells were co-transfected with linearized pVenus-M or -S vectors and TALEN plasmids by electroporation, and single-cell clones were isolated by G418 selection and limiting dilution. Expression of

Venus was analyzed by flow cytometry, and knock-in efficiency was estimated. Venus expression was detected in Jurkat cells transfected with both of the shorter targeting vectors as well as with pVenus-L. However, the frequency of Venus-positive cells among the isolated clones was lower with vectors containing shorter homology arms. Furthermore, the ratio of Venus^{hi} Jurkat cells, which were considered to have random integrations, was increased in cells transduced with shorter targeting vectors. Therefore, the results suggested that the recombination frequency was determined by the length of the homology regions.

Discussion

In this study, we showed that TALEN-mediated genome editing technology could replace an endogenous target gene by using exogenous artificial nucleotides. TALEN-mediated DSB at the target locus has been reported to facilitate HDR by exogenous nucleotides in somatic cells and embryonic stem cells^{21,22,28}. We showed that exogenous nucleotides containing the Venus-Neo cassette were specifically integrated at the *IL2RG* locus (Figure 3). Furthermore, we demonstrated that the efficiency of HDR was dependent on the length of the homology regions used in the gene targeting vector (Table 2).

By using a gene targeting vector along with TALENs, we have succeeded in isolating the knock-in cells with high efficiency. Generation of knock-in cell lines would accelerate the in vitro analysis of gene function in the cell, and would be expected to be applied in various fields. Thus, generation of the cells harboring mutations found in patients would promote the understanding of the disease pathology of each patient.

Gene therapies using viral vectors to introduce therapeutic genes into the genome have not been able to uniquely target the site of gene insertion. Because of this, activation of proto-oncogenes caused by vector-mediated insertional mutagenesis has occurred in some patients, sometimes resulting in the development of leukemia. To reduce the risk of leukemogenesis, site-directed recombination induced by TALEN and vectors containing homology regions of the therapeutic gene is a superior method for replacing a mutant endogenous gene with a functional exogenous cDNA in somatic stem cells. Moreover, expression of the therapeutic gene would be regulated by an endogenous promoter. We found that longer homology regions were required for higher recombination efficiencies (Table 2). The efficiency of recombination at the *IL2RG* locus was quite high (up to 76%), and fewer numbers of cells with random integrations appeared when the longest targeting vector was used (Table 2). The incidence of random integration into the genome indicates that this technology has some limitations that need to be overcome. Some diseases are caused by loss-of-function mutations in regulatory genes, resulting in uncontrolled gene expression that can lead to another disorder. These kinds of diseases are not suitable candidates for vector-mediated gene therapy. However, physiological expression of therapeutic genes achieved by genome editing-mediated gene therapy could treat these diseases. SCID-X1 is thought to be suitable for gene therapy, as lymphocyte progenitor cells with functional *IL2RG* show a selective advantage over defective progenitors. This phenomenon was first observed in a SCID-X1 patient who had a reverse mutation in *IL2RG* that restored gene function²⁹. Gene therapy for diseases in which there is no selective advantage conferred by the transgene, such as chronic granulomatous disorder, is thought to require pre-conditioning of bone marrow to engraft the gene-corrected progenitors³⁰. Therefore, it is important to carefully select candidate diseases for gene therapy.

Disease-causing mutations of *IL2RG* in SCID-X1 patients are not evenly distributed³¹. Precise corrections of the mutation at the single nucleotide level have been reported³². This therapeutic strategy requires the design and construction of custom-made TALENs and targeting vectors for each patient. Although personalized medi-

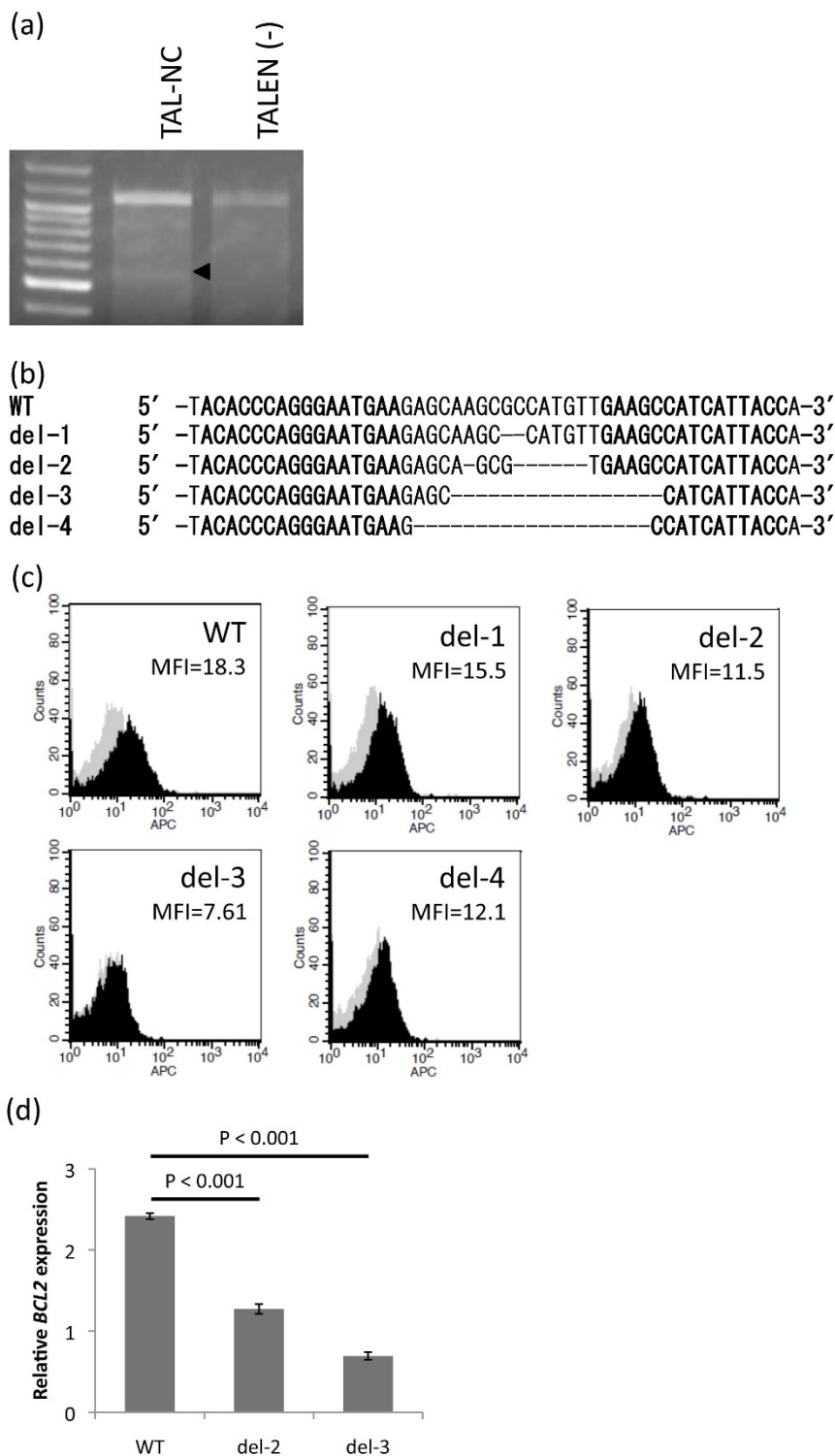


Figure 2 | TALEN-induced genomic mutation in *IL2RG*. (a) T7 endonuclease I assay using TALENs for Jurkat cells. Jurkat cells were transfected with TALEN expression vectors by electroporation. After 5 days culture, genomic DNA was isolated and the TALEN target locus was amplified by PCR. A T7 endonuclease I assay was performed using purified PCR products. The arrowhead indicates the expected position of the digested products in the agarose gel. (b) Sequencing results of the PCR fragments, revealing different mutations in the TALEN target site. Jurkat cells were cultured for 5 days after electroporation, and cloning was performed by limiting dilution. Genomic DNA was isolated from cloned Jurkat cells and DNA sequencing was performed. Sequences for wild-type (WT) and deletion mutants (del1–4) are shown. (c) Functional analysis of genome-modified Jurkat cells. The level of *IL2RG* expression in genome-modified Jurkat cells was analyzed using flow cytometry. Cells were incubated with APC-conjugated-anti-hCD132 antibody for *IL2RG* and APC-IgG2b antibody as an isotype control. MFI, Mean Fluorescence Intensity of CD132. (d) qPCR analysis of *BCL2*. *BCL2* expression was examined 48 hr after the PMA and ionomycin stimulation in the presence of exogenous IL-2. Data are shown as mean ± SD (n = 3).


Table 1 | Efficiency of TALEN-mediated genome modification in Jurkat cells

	Scaffold	Number of clone	Efficiency
Exp. 1	pcDNA-TAL-NC	4/84	4.8%
Exp. 2	pcDNA-TAL-NC	2/15	13.3%

cine is an ideal strategy, this approach is costly and time consuming, also increases the risk of medical errors. By comparison, our strategy could replace mutations by functional cDNA with a single set of TALENs and gene targeting vector (Figure 3).

We showed that the N- and/or C- terminal regions of TALEN are crucial for activity. As shown in Figure 2b and 2c, mutations near the start codon of the *IL2RG* locus resulted in decreased or diminished *IL2RG* expression in TAL-NC-transfected cells. Moreover, mutant cells showed decreased expression of *BCL2* by PMA and ionomycin treatment in the presence of IL-2, indicating that TALEN-mediated loss of *IL2RG* expression leads to functional alteration triggered by IL-2 (Figure 2d). Cloned Jurkat cells transfected with TAL3 TALENs induced mutations to the same extent as that observed in TAL-NC TALEN-transduced cells, while bands from T7 endonuclease digests were barely detectable (data not shown). However, it should be noted that endonuclease *FokI* fused with the TAL3 TALEN differed from that of TAL and TAL-NC. Although normal *FokI* endonuclease functions as a homodimer, mutant *FokI* fused with the TAL3 backbone functions as an obligate heterodimer³³. Thus, it is possible that the lower rate of mutation in TAL3 TALEN-transfected cells was due to reduced nuclease activity. On the other hand, it is assumed that the number of spacer nucleotides (which are inserted between both TALENs) also influenced the induction of mutations, since luciferase activity was higher in TAL-NC TALENs than in TAL TALENs (Figure 1b).

In conclusion, we showed that genome editing by artificial nuclease along with gene targeting vector could be a powerful tool to modify endogenous gene. To carry out clinical applications of genome editing-mediated gene therapy, some problems need to be solved, such as random integration events. For gene replacement in hematopoietic stem cells, this issue could be addressed with a screening system that removes random knock-in clones and off-target mutated clones, or a system based on positive-selection of targeted knock-in clones.

Methods

TALEN and targeting-vector construction. All of TALEN vectors used in this study were obtained from Addgene. The pair of TALENs recognizing human *IL2RG* was designed using ZiFiT³⁴. TALE repeats were constructed using the Golden Gate TALEN assembly method as described previously, with some modifications²⁴. The module plasmids were *BsaI* digested, and fragments encoding RVD-specific sequences were purified in advance by gel electrophoresis. RVDs were cloned into array plasmids by using a DNA Ligation Kit (Takara, Shiga, Japan). Screening of assembled clones by colony PCR and cloning of the constructed array plasmid and the appropriate last repeat into mammalian expression vectors (pcDNA-TAL, pcDNA-TAL-NC, or pcDNA-TAL3) by using the Golden Gate method were performed as described previously²⁴. Each plasmid or vector was transformed into *Escherichia coli* DH5 α competent cells.

The pVenus vector was used as the backbone to construct the *IL2RG*-targeting vector pVenus-L. A 5662 bp 5' homology arm and a 3000 bp 3' homology arm were amplified by PCR from the Jurkat cell genome, and cloned into the pVenus by using a DNA Ligation Kit. Donor DNA was linearized by *Eam1105I* or *KpnI* digestion and purified by gel electrophoresis. Targeting vectors with various arm lengths were obtained following the same strategy. Homology arms were amplified by PCR from pVenus-L, and cloning was performed with GeneArt Seamless Cloning and Assembly Enzyme Mix (Life Technologies, Carlsbad, CA).

Single-strand annealing (SSA) assay. The SSA assay was performed as previously described²⁴. HEK293T cells were cultured in DMEM supplemented with 10% fetal bovine serum (FBS) (Hana-Nesco Bio Corp, Tokyo, Japan). Cells (4.4×10^4 were co-transfected with 400 ng of each of the TALEN expression plasmids, 200 ng of the pGL4-SSA reporter plasmid, and 40 ng of the pRL-TK reference vector using Polyethylenimine "Max" (Polysciences, Warrington, PA) in a 48-well plate. After

48 h, dual-luciferase assays were carried out using the Dual-Glo luciferase assay system (Promega, Madison, WI) in a ARVO X3 Multilabel Plate Reader (PerkinElmer, Waltham, MA) following the manufacturer's instructions. pGL4-SSA reporter plasmids were constructed as previously described²⁴.

Cell culture and transfection. Jurkat cells were maintained in RPMI-1640 medium (Sigma, St. Louis, MO) supplemented with 10% FBS, 55 μ M 2-mercaptoethanol (Life Technologies, Carlsbad, CA), 5 mM HEPES, 1 mM sodium pyruvate (Nacalai Tesque, Kyoto, Japan), 100 U/mL penicillin, and 100 μ g/mL streptomycin at 37°C with 5% CO₂ incubation. Jurkat cells were transfected by electroporation by using a Nepa21 pulse generator (Nepa Gene, Chiba, Japan). Jurkat cells were suspended in OPTI-MEM (Life Technologies) at a density of 2×10^5 cells per electrode chamber with 10 μ g each of Left TALEN vector and Right TALEN vector and placed in an electrode chamber. For targeted knock-in through homologous recombination, 2 μ g of the targeting vector was added. Two rectangular electric pulses (150 V, 5-ms duration, 50-ms interval, decay constant: 10%), followed by five pulses (20 V, 50-ms duration, 50-ms interval, decay constant: 40%) and another five pulses in the opposite direction of the electric field were delivered. G418 (Nacalai Tesque) at 500 μ g/ml was added to the medium 4 d after transfection for selection of targeted knock-in clones. Single-cell clones of genome-modified Jurkat cells and targeted knock-in Jurkat cells were obtained by limiting dilution.

T7 Endonuclease I assay. The T7 Endonuclease I assay was performed as previously described³⁵. Jurkat cells were cultured and transfected as described above. Five days after transfection, genomic DNA was isolated from cells transfected with TALEN-encoding or control plasmids using the DNeasy Blood & Tissue Kit (Qiagen, Hilden, Germany) according to the manufacturer's instructions. Endogenous loci were amplified by PCR using the following primers: Forward (5'-GGA CCC AGC TCA GGC AGC A-3') and Reverse (5'-TGG GCA TAG TGG TCA GGA AGA-3'). PCR products were purified with the QIAquick PCR Purification Kit (Qiagen) according to manufacturer's instructions. Purified PCR product (200 ng) was denatured and reannealed in NE Buffer 2 (New England Biolabs, Ipswich, MA) using a thermocycler with the following protocol: 95°C, 5 min; 95–85°C at –2°C/s; 85–25°C at –0.1°C/s; hold at 4°C. Hybridized PCR products were treated with 10 U of T7 Endonuclease I (New England Biolabs) at 37°C for 15 min in a reaction volume of 20 μ l. Reactions were stopped by the addition of 2 μ l of 0.5 M EDTA, and gel electrophoresis of the products was performed.

Sequencing analysis for genome modification. Genomic DNA was extracted using the DNeasy Blood & Tissue Kit (Qiagen) following the manufacturer's protocol. Genomic regions surrounding the TALEN target site were amplified by PCR using the following primers: Forward (5'-CAC CCT CTG TAA AGC CCT GG-3') and Reverse (5'-CCA GTC CCA GAT TTC CCA CC-3'). PCR products were purified using the QIAquick PCR Purification Kit according to the manufacturer's protocol. DNA sequencing was performed by general Sanger method.

Flow cytometry. APC-conjugated anti-human CD132 (clone: TUGh4) and APC-Rat IgG2b, k Isotype ctrl (clone: RTK4530) (BioLegend, San Diego, CA) antibodies were used for flow cytometry analyses of genome-modified Jurkat cells. Flow cytometry was performed on a FACSCalibur HG flow cytometer with CELL Quest Pro software (Becton Dickinson, Franklin Lakes, NJ). Dead cells were excluded by gating of forward and side scatter.

Jurkat cell stimulation. Jurkat cells (1×10^6 cells/ml) were stimulated with the indicated concentrations of PMA (100 ng/ml; Sigma), ionomycin (1 μ g/ml; Sigma) and IL-2 (100 ng/ml; BioLegend) for 48 hr in 24-well plates. We chose five cloned Jurkat cells which had no mutations in *IL2RG* as wild-type control, at random.

Quantitative PCR. Total cell RNA from Jurkat cells were isolated using ISOGEN (Nippon Gene, Tokyo, Japan) following the manufacturer's protocol. We used 2 μ g purified RNA to synthesize the first strand of cDNA with SuperScript II Reverse Transcriptase (Life Technologies), and diluted 1:20 prior to the Quantitative PCR (qPCR) analysis.

qPCR was performed using Power SYBR green PCR master mix (Applied Biosystems Inc. Foster City, CA) and the following primers: *BCL2* Forward (5'-GAC TGA GTA CCT GAA CCG GC-3'), *BCL2* Reverse (5'-AGT TCC ACA AAG GCA TCC CAG-3'), *ACTB* Forward (5'-CCC CGC GAG CAC AGA G-3') and *ACTB* Reverse (5'-ATC ATC CAT GGT GAG CTG GC-3'). All qPCRs were performed in triplicates. Results were normalized to β -actin, and then calculated relative to non-stimulated cells, respectively.

Southern blot analysis. Following electrophoresis, gels were immersed in denaturation buffer (0.5 M NaOH, 1.5 M NaCl) for 30 min, followed by neutralization buffer (0.5 M Tris-HCl [pH 7.5], 1.5 M NaCl) for 10 min. Capillary transfer of DNA from agarose gels to nylon membranes (Amersham Hybond-N+, GE Healthcare, Buckinghamshire, United Kingdom) was conducted overnight with 20 \times SSC buffer (3 M NaCl, 300 mM sodium citrate, pH 7.0). Transferred DNA was fixed on membranes by UV irradiation and air-dried. Membranes were pre-incubated in hybridization buffer (DIG Easy Hyb; Roche, Basel, Switzerland) at 48°C for 30 min. The solution of DIG-labeled DNA probe was generated with the PCR DIG Probe Synthesis Kit (Roche) following the manufacturer's protocol. To generate the probe, PCR was performed using the following primers: Forward (5'-AGT CAC

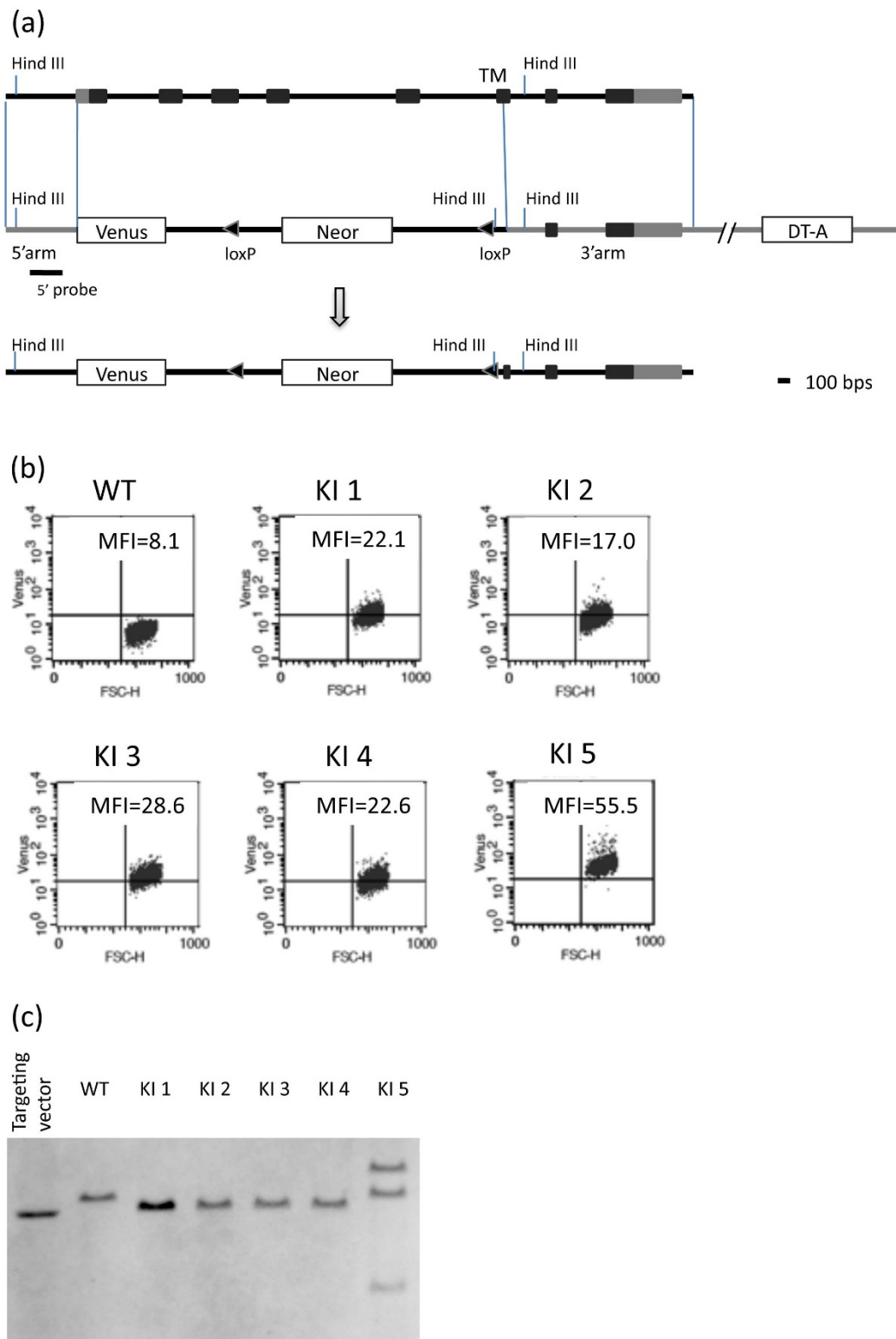


Figure 3 | TALEN-mediated genome editing. (a) *Top*: Schematic of the endogenous *IL2RG* locus. *HindIII*, *HindIII* restriction sites used for Southern blot analysis; TM, transmembrane domain. *Middle*: Schematic of the targeting vector. The targeting vector contained Venus cDNA, lox-P-flanked Neomycin resistance cassette, and DT-A negative selectable marker. The 5' homology arm upstream of the *IL2RG* start codon was cloned upstream of Venus cDNA, and the 3' homology arm downstream of the *IL2RG* transmembrane sequence (exon 6) was cloned downstream of the Neomycin resistance cassette (Neor). 5' probe, Probe used for Southern blot analysis. *Bottom*: Schematic of the targeted *IL2RG* locus. A novel *HindIII* restriction site would introduced when the targeted knock-in was successful. (b) Flow cytometric analysis of Venus in Jurkat cells with targeted knock-in of *IL2RG*. Each Jurkat cell clone was analyzed for YFP fluorescence expressed from knocked-in Venus cDNA. WT, wild-type Jurkat cells; KI 1-4, individual clones with targeted knock-in; KI 5, Venus^{hi}, MFI, Mean Fluorescence Intensity of Venus. (c) Southern blot analysis of Jurkat cells with targeted knock-in of *IL2RG*. *HindIII* digestion resulted in a 3788 bp band from the WT endogenous *IL2RG* locus and a 3515 bp band (containing Venus cDNA and the Neomycin resistance cassette) from the targeted knock-in. Targeting vector was used as positive control for targeted knock-in, and genomic DNA isolated from WT Jurkat cells was used as negative control.



Table 2 | Results of *IL2RG* knock-in (KI) experiments in Jurkat cells, showing the correlation between homology arm length of the TALEN vector and percentage efficiency of recombination at the *IL2RG* locus

pVenus ^a	5' arm [bp]	3' arm [bp]	Targeted KI ^b	Random KI ^b
L	5.6 k	3.0 k	76.0% (38/50)	24.0% (12/50)
M	3.0 k	2.0 k	53.3% (32/60)	46.7% (28/60)
S	1.0 k	1.0 k	39.5% (15/38)	60.5% (23/38)

^a L, M, and S refer to long, medium, and short homology arm lengths, respectively, in bp × 1000 (k).

^b Percent efficiency of *IL2RG*-targeted or random integration of TALEN vectors was determined from the values shown in parentheses using the formula: (number of positive clones/total number of clones analyzed) × 100.

ACT TCC TCG CCA GT-3') and Reverse (5'-ACC CAC ACG TTT CCT CTG TC-3'). The probe was heated at 95°C for 5 min and chilled quickly in ice, then diluted 500-fold with hybridization buffer. Membranes were incubated overnight with the diluted probe solution at 48°C. Membranes were washed twice at room temperature for 5 min with 2× SSC and 0.1% SDS, and twice at 68°C for 15 min with 0.1× SSC and 0.1% SDS. Subsequently, membranes were washed with washing buffer (0.1 M maleic acid/NaOH [pH 7.5], 0.15 M NaCl, and 0.3% Tween 20) for 2 min and incubated with blocking buffer (Blocking Reagent, Roche) for 30 min. Membranes were then incubated with 75 mU/ml Anti-Digoxigenin-AP Fab fragments (Roche) in blocking buffer at room temperature for 30 min and washed twice for 15 min with washing buffer. Finally, membranes were incubated with CDP-Star chemiluminescent substrate (Roche) at room temperature for 5 min, followed by incubation with reaction buffer (0.1 M Tris-HCl, 0.1 M NaCl, pH 9.5) for 3 min. Digital images of membranes were obtained using the ImageQuant LAS 4000 mini imaging system (GE Healthcare).

Statistical analysis. For all statistical analysis, two-tailed Student's t-tests were performed using Excel spreadsheet. p values are given for each individual experiment.

- Noguchi, M. *et al.* Interleukin-2 receptor gamma chain mutation results in X-linked severe combined immunodeficiency in humans. *Cell* **73**, 147–157 (1993).
- Sugamura, K. *et al.* The interleukin-2 receptor gamma chain: its role in the multiple cytokine receptor complexes and T cell development in XSCID. *Annu. Rev. Immunol.* **14**, 179–205 (1996).
- Cavazzana-Calvo, M. *et al.* Gene therapy of human severe combined immunodeficiency (SCID)-X1 disease. *Science* **288**, 669–672 (2000).
- Gaspar, H. B. *et al.* Gene therapy of X-linked severe combined immunodeficiency by use of a pseudotyped gammaretroviral vector. *Lancet* **364**, 2181–2187 (2004).
- Hacein-Bey-Abina, S. *et al.* Efficacy of gene therapy for X-linked severe combined immunodeficiency. *N. Engl. J. Med.* **363**, 355–364 (2010).
- Hacein-Bey-Abina, S. *et al.* A Serious Adverse Event after Successful Gene Therapy for X-Linked Severe Combined Immunodeficiency. *N. Engl. J. Med.* **348**, 255–256 (2003).
- Hacein-Bey-Abina, S. *et al.* LMO2-Associated Clonal T Cell Proliferation in Two Patients after Gene Therapy for SCID-X1. *Science* **302**, 415–419 (2003).
- Hacein-Bey-Abina, S. *et al.* Insertional oncogenesis in 4 patients after retrovirus-mediated gene therapy of SCID-X1. *J. Clin. Invest.* **118**, 3132–3142 (2008).
- Kohn, D. B., Sadelain, M. & Glorioso, J. C. Occurrence of leukaemia following gene therapy of X-linked SCID. *Nat. Rev. Cancer.* **3**, 477–488 (2003).
- Bushman, F. D. Retroviral integration and human gene therapy. *J. Clin. Invest.* **117**, 2083–2086 (2007).
- Deichmann, A. *et al.* Vector integration is nonrandom and clustered and influences the fate of lymphopoiesis in SCID-X1 gene therapy. *J. Clin. Invest.* **117**, 2225–2232 (2007).
- Schwarzwaelder, K. *et al.* Gammaretrovirus-mediated correction of SCID-X1 is associated with skewed vector integration site distribution in vivo. *J. Clin. Invest.* **117**, 2241–2249 (2007).
- Yáñez, R. J. & Porter, A. C. Therapeutic gene targeting. *Gene Ther.* **5**, 149–159 (1998).
- Chapman, J. R., Taylor, M. R. & Boulton, S. J. Playing the end game: DNA double-strand break repair pathway choice. *Mol. Cell* **47**, 497–510 (2012).
- Kim, Y. G., Cha, J. & Chandrasegaran, S. Hybrid restriction enzymes: zinc finger fusions to Fok I cleavage domain. *Proc. Natl. Acad. Sci. U S A.* **93**, 1156–1160 (1996).
- Bibikova, M., Beumer, K., Trautman, J. K. & Carroll, D. Enhancing gene targeting with designed zinc finger nucleases. *Science* **300**, 764 (2003).
- Urnov, F. D. *et al.* Highly efficient endogenous human gene correction using designed zinc-finger nucleases. *Nature* **435**, 646–651 (2005).

- Urnov, F. D., Rebar, E. J., Holmes, M. C., Zhang, H. S. & Gregory, P. D. Genome editing with engineered zinc finger nucleases. *Nat. Rev. Genet.* **11**, 636–646 (2010).
- Christian, M. *et al.* Targeting DNA double-strand breaks with TAL effector nucleases. *Genetics* **186**, 757–761 (2010).
- Miller, J. C. *et al.* A TALE nuclease architecture for efficient genome editing. *Nat. Biotechnol.* **29**, 143–148 (2011).
- Bedell, V. M. *et al.* In vivo genome editing using a high-efficiency TALEN system. *Nature* **491**, 114–118 (2012).
- Zu, Y. *et al.* TALEN-mediated precise genome modification by homologous recombination in zebrafish. *Nat. Methods* **10**, 329–331 (2013).
- Schneider, U., Schwenk, H. U. & Bornkamm, G. Characterization of EBV-genome negative “null” and “T” cell lines derived from children with acute lymphoblastic leukemia and leukemic transformed non-Hodgkin lymphoma. *Int. J. Cancer* **19**, 621–626 (1977).
- Akbar, A. N. *et al.* Interleukin-2 receptor common gamma-chain signaling cytokines regulate activated T cell apoptosis in response to growth factor withdrawal: selective induction of anti-apoptotic (*bcl-2*, *bcl-x_L*) but not pro-apoptotic (*bax*, *bcl-x_S*) gene expression. *Eur. J. Immunol.* **26**, 294–299 (1996).
- Ding, Q. *et al.* Enhanced efficiency of human pluripotent stem cell genome editing through replacing TALENs with CRISPRs. *Cell Stem Cell* **12**, 393–394 (2013).
- Bouso, P. *et al.* Diversity, functionality, and stability of the T cell repertoire derived in vivo from a single human T cell precursor. *Proc. Natl. Acad. Sci. U S A.* **97**, 274–278 (2000).
- Nagai, T. *et al.* A variant of yellow fluorescent protein with fast and efficient maturation for cell-biological applications. *Nat. Biotechnol.* **20**, 87–90 (2002).
- Grez, M., Reichenbach, J., Schwäble, J., Seger, R., Dinauer, M. C. & Thrasher, A. J. Gene therapy of chronic granulomatous disease: the engraftment dilemma. *Mol. Ther.* **19**, 28–35 (2011).
- Puck, J. M. *et al.* Mutation analysis of *IL2RG* in human X-linked severe combined immunodeficiency. *Blood* **89**, 1968–1977 (1997).
- Yusa, K. *et al.* Targeted gene correction of α 1-antitrypsin deficiency in induced pluripotent stem cells. *Nature* **478**, 391–394 (2011).
- Dahlem, T. J. *et al.* Simple methods for generating and detecting locus-specific mutations induced with TALENs in the zebrafish genome. *PLoS Genet.* **8**, e1002861 (2012).
- Sander, J. D. *et al.* ZinFiT (Zinc Finger Targeter): an updated zinc finger engineering tool. *Nucleic Acids Res.* **38**, W462–468 (2010).
- Cermak, T. *et al.* Efficient design and assembly of custom TALEN and other TAL effector-based constructs for DNA targeting. *Nucleic Acids Res.* **39**, e82 (2011).
- Sakuma, T. *et al.* Efficient TALEN construction and evaluation methods for human cell and animal applications. *Genes Cells* **18**, 315–326 (2013).
- Reyon, D. *et al.* FLASH assembly of TALENs for high-throughput genome editing. *Nat. Biotechnol.* **30**, 460–465 (2012).

Acknowledgments

This work was supported in part by The Grant of National Center for Child Health and Development, Grant Number 25-1, JSPS KAKENHI Grant Number 24115707, 24659669, 23249071, JST (CREST), NIH grant AR050631, Bristol-Myers RA Research Fund, and Mochida Memorial Fund to H.A.

Author contributions

Y.M. performed the experiments, analyzed the data, drafted and approved the manuscript. T.C. designed the experiments, analyzed the data, drafted and approved the manuscript. K.K., T.M. and S.M. approved the manuscript. S.T. established the protocol for TALEN construction and approved the manuscript. H.A. designed the experiments, drafted and approved the manuscript.

Additional information

Supplementary information accompanies this paper at <http://www.nature.com/scientificreports>

Competing financial interests: The authors declare no competing financial interests.

How to cite this article: Matsubara, Y. *et al.* Transcription activator-like effector nuclease-mediated transduction of exogenous gene into *IL2RG* locus. *Sci. Rep.* **4**, 5043; DOI:10.1038/srep05043 (2014).



This work is licensed under a Creative Commons Attribution-NonCommercial-NoDerivs 3.0 Unported License. The images in this article are included in the article's Creative Commons license, unless indicated otherwise in the image credit; if the image is not included under the Creative Commons license, users will need to obtain permission from the license holder in order to reproduce the image. To view a copy of this license, visit <http://creativecommons.org/licenses/by-nc-nd/3.0/>